Theoretical Study of the Reaction $O(^3P)$ + 1,2-Butadiene

Gianmarco Vanuzzo[1(✉)], Andrea Giustini[1], Marzio Rosi[2], Piergiorgio Casavecchia[1], and Nadia Balucani[1]

[1] Department of Chemistry, Biology and Biotechnology, University of Perugia, 06123 Perugia, Italy
{gianmarco.vanuzzo,andrea.giustini,piergiorgio.casavecchia, nadia.balucani}@unipg.it
[2] Department of Civil and Environmental Engineering, University of Perugia, 06125 Perugia, Italy
marzio.rosi@unipg.it

Abstract. The triplet and singlet potential energy surfaces of the $O(^3P)$ + 1,2-butadiene reaction have been investigated by electronic structure calculations at the coupled-cluster (CCSD(T)(aug-cc-pVTZ) level. We focused our attention, in particular, on the different sites of attack of atomic oxygen to 1, 2-butadiene. The results for minima, transition states and reaction channel energetics are compared with the results of previous CCSD(T)(aug-cc-pVTZ)-CBS and CASPT2 calculations to explore the adequacy of simpler computational schemes for discussing the reaction dynamics, in particular the product branching fractions derived from crossed molecular beam experiments.

Keywords: Ab initio calculations · Reaction dynamics of oxygen atoms with dienes · Combustion chemistry

1 Introduction

The reactions between ground state atomic oxygen, $O(^3P)$, and aliphatic unsaturated hydrocarbons (UHs) play a critical role in combustion chemistry [1–4], and are important in the chemistry of the terrestrial atmosphere [4, 5]. In addition, these reactions are also of some relevance in astrochemistry [6, 7]. In combustion processes, such as fuel oxidation, $O(^3P)$ is generated from what is considered to be the most important reaction in combustion chemistry, namely, $O_2 + H \rightarrow O(^3P) + OH$, and generally is produced in all oxygen-rich environments [3, 4]. On the other hand, small UHs are formed during the combustion of both simple, such as methane, and complex fossil fuels, including biofuels. If both UHs and $O(^3P)$ coexist in the same environment, reactions between these species can occur. Among the different molecules formed during these processes, carbon dioxide is the most important one, because it remains indefinitely in our atmosphere. For this reason, CO_2 is considered the main by-product of fossil fuel combustion [1–5]. To cut down on the overproduction of CO_2, numerous car manufacturers, utility

© The Author(s), under exclusive license to Springer Nature Switzerland AG 2022
O. Gervasi et al. (Eds.): ICCSA 2022 Workshops, LNCS 13382, pp. 249–263, 2022.
https://doi.org/10.1007/978-3-031-10592-0_19

companies, and governments have been pursuing new alternatives for energy sources. Among the leading contenders, there are new substances, the so-called *biofuels*, made from biological materials, that are considered as renewable energy sources. Among the various biofuels, the two most common that can replace gasoline are ethanol and biodiesel, where the former is mainly extracted from corn or sugarcane [1, 2, 4], while the latter is a plant/animal-based substance produced through the trans-esterification process of vegetal oil or animal fats [1]. Combustion and pyrolysis of biofuels can lead to formation of unsaturated hydrocarbons [1, 2, 4, 8]. Hence, studies of the reactions between $O(^3P)$ and UHs are useful for better understanding the kinetics and improve the modeling of combustion environments.

Since the reactions of $O(^3P)$ with UHs are particularly relevant in the global understanding of the complex mechanisms involved in combustion chemistry, the kinetics and dynamics of these processes have been investigated in depth from both experimental [5, 9–15] and theoretical [16–23] points of view. For instance, since the 1950s the global rate constants at room temperature have been determined in kinetic experiments for many of these reactions [9], and in some cases also in a range of combustion temperatures [8]. In contrast, much less is known about the identity of the primary reaction products and their relative yields (branching fractions, BFs), with the latter having often been object of uncertainty and controversy [19, 24, 25]. The difficulty in determining the product BFs is caused by the complexity of the $O(^3P)$ + UH reactions [10]. In fact, these processes are multichannel reactions, characterized by numerous thermodynamically accessible product channels. Furthermore, in these systems, nonadiabatic transitions from the entrance triplet to the underlying singlet potential energy surface (PES), namely the occurrence of *intersystem crossing* – ISC, can open other reaction channels [10, 12, 25, 27, 30]. We recall that the knowledge of both global rate constants and relative product yields are fundamental for the global understanding of these processes and for the improvement of combustion models [8], because the primary products of one elementary reaction are, basically, the reactants of the following processes in the overall combustion network, and, therefore, can determine the propagation or the termination of the chain reaction. Traditionally, only partial information on BFs has become available from kinetic studies; furthermore, not only the kinetic data available are partial, but they have been obtained mostly at room temperature, that is, far from typical combustion conditions. As a result, most combustion mechanisms describe the high temperature reactivity of $O(^3P)$ with UHs using the total rate constant partitioned in the various reaction channels based on the very limited room temperature BFs, and this can lead to substantial errors. When data are not available at all, reaction products are normally guessed by considering as most probable the most exothermic reaction channels, or by drawing analogies with similar systems, but again both approaches can be wrong [see ref. 12, 30, 31, and references therein]. In the case of multichannel reactions, such as those of $O(^3P)$ with UHs, in general the primary products are not easy to predict, because the characteristics of the underlying triplet and singlet PESs are those that govern the relative yield of the various product channels. In addition, the occurrence of ISC and its extent as a function of temperature are not easy to predict either, and only experimental determinations and/or accurate theoretical treatments can quantify it. So, there is a strong need for accurate

experimental data on product BFs at the temperature (or energy) of relevance in combustion that support theoretical predictions. Importantly, the experimental results can be used to validate the reliability of the statistical predictions of product BFs, and hence of the calculated triplet and singlet PESs and their nonadiabatic couplings. Once theory is validated by experiment, it can be used with confidence to calculate channel-specific rate constants and BFs for all energetically allowed product channels as a function of temperature and pressure, which is what is needed for theoretical modelling (see, for instance, refs. 12, 26, 30, and 31).

During the past 15 years, in our laboratory the study of numerous multichannel reactions of $O(^3P)$ with UHs was performed using the crossed-molecular-beam technique with mass-spectrometric detection (CMB-MS), empowered with *soft* electron ionization (EI), which allowed us to identify and quantify all primary reaction products. Using *soft* EI we were, in fact, able to mitigate or even suppress the dissociative ionization of interfering species (products, background gases, and, in particular, elastically/inelastically scattered reagents) that occurs when an electron energy of 70 eV is used in the EI source (*hard* ionization), and which usually represents the main complication in these experiments [29]. Among the various UHs, we have investigated the oxidation of molecules with different degree of unsaturation and complexity, starting from alkenes [11, 12, 21, 24–26], and moving to cumulenes [11, 14, 27], alkynes [11, 14, 15, 28, 29], and also aromatics (benzene) [30, 45] and conjugated dienes (1, 3-butadiene) [31].

It should be noted that the oxidation of dienes, such as allene (propadiene), the prototype of cumulenes, is possible through three different sites of oxygen attack, where the terminal ones are equivalent. Previous CMB studies from our laboratory on the $O(^3P)$ + allene ($CH_2 = C = CH_2$) reaction at the collision energy, E_c, of 39.3 kJ/mol found that it is characterized by numerous product channels, where the dominant one is C_2H_4 + CO (BF = 0.77), followed by $H_2CO + C_3H_4$ (BF = 0.091), $CH_3CO + CH_2$ (BF = 0.065), $HCO + C_2H_3$ (BF = 0.062), and $CH_2COCH + H$ (BF = 0.015) [27]. On the basis of these experimental results, it was concluded that the $O(^3P)$ + allene reaction is dominated by ISC (–90%) because the main primary products, namely CO, HCO, and H_2CO can only originate via ISC from the entrance triplet to the lowest singlet PES. Notably, the above BFs were in line with statistical predictions of earlier *ab initio* and statistical (RRKM) calculations performed by Nguyen *et al.* [23] separately on the triplet and singlet PESs (that is, ISC was not included in the statistical calculations).

Recently, in our laboratory also the reaction $O(^3P)$ + 1,2-butadiene (methylallene) was studied by a combined CMB and theoretical approach. While a preliminary report has been already published [32], more theoretical work is needed for a detailed understanding of the reaction mechanism and of the product BFs derived from the CMB experiments.

We recall that the energetically allowed reaction channels of $O(^3P)$ + methylallene are the following:

$$O(^3P) + CH_2{=}C{=}CH - CH_3 \rightarrow C_4H_5O + H \quad \Delta H_0^0 = -54 \quad \text{kJ/mol} \tag{1}$$

$$\rightarrow C_4H_4O + H_2 \quad \Delta H_0^0 = -335 \quad \text{kJ/mol} \tag{2}$$

$$\rightarrow CO + C_3H_6 \quad \Delta H_0^0 = -504 \quad \text{kJ/mol} \tag{3}$$

$$\rightarrow \mathrm{OH} + \mathrm{C_4H_5}\ \Delta \mathrm{H}_0^0 = -59\ \ \mathrm{kJ/mol} \tag{4}$$

$$\rightarrow \mathrm{C_3H_3O} + \mathrm{CH_3}\ \Delta \mathrm{H}_0^0 = -95\ \ \mathrm{kJ/mol} \tag{5}$$

$$\rightarrow \mathrm{H_2CO} + \mathrm{C_3H_4}\ \Delta \mathrm{H}_0^0 = -326\ \ \mathrm{kJ/mol} \tag{6}$$

$$\rightarrow \mathrm{HCCO} + \mathrm{C_2H_5}\ \Delta \mathrm{H}_0^0 = -103\ \ \mathrm{kJ/mol} \tag{7}$$

$$\rightarrow \mathrm{HCO} + \mathrm{C_3H_5}\ \Delta \mathrm{H}_0^0 = -202\ \ \mathrm{kJ/mol} \tag{8}$$

$$\rightarrow \mathrm{CH_3CO} + \mathrm{C_2H_3}\ \Delta \mathrm{H}_0^0 = -127\ \ \mathrm{kJ/mol} \tag{9}$$

$$\rightarrow \mathrm{CH_2CHO} + \mathrm{C_2H_3}\ \Delta \mathrm{H}_0^0 = -98\ \ \mathrm{kJ/mol} \tag{10}$$

$$\rightarrow \mathrm{CH_2CO} + {}^3\mathrm{CHCH_3}\ \Delta \mathrm{H}_0^0 = -109\ \ \mathrm{kJ/mol} \tag{11}$$

$$\rightarrow \mathrm{CH_2CO} + {}^1\mathrm{CH_2CH_2}\ \Delta \mathrm{H}_0^0 = -444\ \ \mathrm{kJ/mol} \tag{12}$$

where the reaction enthalpies are obtained from the standard enthalpies of formation from NIST [33] or from our previous [32] and current electronic structure calculations.

In our preliminary work [32], the C_4H_6O triplet PES was investigated in a synergistic manner combining density functional theory (DFT), coupled cluster with perturbative triple excitations (CCSD(T)) with complete basis set (CBS) extrapolation, and multireference CASPT2 calculations, while the singlet PES was not explicitly investigated; in particular, the energy barriers regarding the isomerization processes of the oxiranyl singlet intermediate to aldehydes were assumed to be the same as those calculated for propene oxide isomerization to propenal [26].

In the present paper, we have extended the theoretical investigation of the triplet and singlet PESs of the $O(^3P)$ + 1,2-butadiene reaction by calculating minima, barriers, and reaction enthalpies at the coupled-cluster (CCSD(T)(aug-cc-pVTZ) level. The goal was to compare the CCSD(T) results with those from the previous CCSD(T)-CBS and CASPT2 results, to explore whether a much faster scheme of electronic structure calculations were sufficiently reliable for future statistical RRKM/ME (Rice-Ramsperger-Kassel-Marcus/Master Equation) calculations of product BFs, to be compared with experimental BFs at the E_c of the CMB experiment. We stress that the inter-conversion barriers between the singlet minima were not available previously for $O(^3P)$ + 1,2-butadiene. This is expected to allow us to expand the interpretation of the experimental results and to also discuss some similarities and differences between the dynamics of the O + allene and O + methylallene (1,2-butadiene) reactions, including the relative extent of ISC.

2 Methods

2.1 Experimental

We have studied the title reaction at the collision energy, E_c, of 41.8 kJ/mol using the CMB method, as described in ref. 32. From product angular and time-of-flight (TOF) distributions at different mass-to-charge (*m/z*) ratios it was experimentally found that the title reaction is characterized by a large variety of sizeable competing reaction channels, of which some lead to radical products, while others to molecular products. In total, nine different product channels were characterized, specifically the channels (1), (2), (3), (5), (6), (8), (9), (10), and (11). In the previous publication [32] we focused on two main molecular channels, both involving the rupture of the carbon backbone of 1,2-butadiene; specifically on channel (3), leading to CO + propene, occurring on the singlet PES (via ISC), and on channel (11) leading to CH_2CO (ketene) + CH_3CH (ethylidene), occurring on the triplet PES. The detailed analysis and discussion of the dynamics of the nine observed channels will be reported in a future, comprehensive publication [34].

2.2 Computational Details

Quantum chemical calculations were carried out to allocate minima and first-order saddle points on both the triplet and the singlet PESs, which have been identified to characterize the reaction O(^{3}P) + 1,2-butadiene. All geometries were optimized by using the Density Functional Theory (DFT) with the wB97XD functional [35, 36] and the aug-cc-pVTZ basis set [37–39]. With respect to our previous calculations [32] this DFT method showed significant improvements in the treatment of the long-range interactions, while similarities have been obtained for bonded interactions. Intrinsic reaction coordinate (IRC) calculations were performed to verify that the transition states are connected to the corresponding reactants and products [40, 41]. In order to refine the energetics of the critical points on the corresponding PESs, the coupled cluster CCSD(T)/aug-cc-pVTZ method was thoroughly adopted afterward. Both the wB97XD and CCSD(T) energies were corrected to 0 K by adding the zero-point energy correction computed using the scaled harmonic vibrational frequencies evaluated at the wB97XD/aug-cc-pVTZ level. Since the accuracy of our best computed values should not be smaller than the "chemical accuracy" of 1 kcal/mol, we rounded all the reported energies to 1 kJ/mol. As regards the energies of the entrance channels we used the values obtained by Caracciolo et al. and reported in reference [32]. DFT calculations were performed using the Gaussian 09 software [42], while all other calculations were performed using Molpro 2021.2 [43, 44].

3 Results and Discussion

Our previous theoretical investigation on the O(^{3}P) + 1,2-butadiene reaction reported three possible sites for the attack of atomic oxygen to the $CH_2 = C = CH\text{-}CH_3$ molecule, namely the terminal carbon of the unsaturated bond (C1), the central carbon between the cumulated double bonds (C2), and the terminal carbon linked to the methyl group

(C3) [32]. A kinetic investigation, based on variational transition state theory (VTST), determined the rate constants for O(^{3}P) addition to the C1, C2, and C3 carbon atoms, and revealed that those to C2 and C3 are the most probable sites of addition (49.0% and 36.3%, respectively), being these addition processes barrierless. In contrast, the presence of an entrance barrier of 2.2 kJ/mol for the C1 addition leads to a lower probability of attack (14.7%). In the Figs. 1, 2, and 3 are reported the schematic representations of the three partial PESs (both triplet and singlet) obtained for the different sites of attack, with the energies evaluated in the present work at the CCSD(T)/aug-cc-pVTZ level of theory, with the exception of the entrance barriers which are taken from the previous calculations at the CASPT2 level.

The addition of O(^{3}P) to the C1 site of CH_2CCHCH_3 features a barrier in the entrance channel, located (at the CASPT2 level [32]) 2.2 kJ/mol above the energy of the reactants, and leads to the formation of the ^{3}W4 intermediate, in which a new C-O bond is formed (see Fig. 1). The fission of a C-H bond in the newly formed triplet intermediate (located 112 kJ/mol below the reactant energy asymptote), allows the formation of atomic hydrogen plus the $CH_3CHCCHO$ radical (channel (1)). The global exothermicity for the process is 44 kJ/mol, and a barrier of 97 kJ/mol must be overcome from ^{3}W4. The related exit transition state (^{3}TS4) (see Fig. 4) clearly shows the breaking of a C-H bond, with a bond distance increasing up to 1.758 Å (see Fig. 4). The exit barrier is then 29 kJ/mol with respect to products. In competition, a nonadiabatic transition (near ^{3}W4) to the singlet PES can take place, through a triplet-to-singlet ISC (see Fig. 1) leading to the ^{1}W7 cyclic intermediate, located 357 kJ/mol below the reactant asymptote. By analogy with the reaction O(^{3}P) + allene, ^{1}W7 can isomerize to ^{1}W8 by ring opening and H migration via the saddle point ^{1}TS7. Unfortunately, at the present level of calculations we were not able to identify the corresponding stationary point; therefore, we have reported the isomerization path from ^{1}W7 to ^{1}W8 in Fig. 1 with blue dashed-lines, where the energy value of the transition state ^{1}TS7 is expected to be comparable to that (-139.7 kJ/mol, in square parenthesis) of the reaction O(^{3}P) + propene [26]. Once formed, the W8 intermediate, which shows a relative energy of –487 kJ/mol, can directly dissociate to HCO + CH_3CHCH (channel (8)), via a barrierless process. Competitively, two isomerization processes can take place: (*i*) The migration of a hydrogen atom from C4 to C2 leading to the formation of the ^{1}W9 intermediate, located 469 kJ/mol below the reactants, overcoming a barrier of 374 kJ/mol (from ^{1}W8); (*ii*) A C1-C2 hydrogen shift, together with the simultaneous formation of a new C-C σ bond, is responsible for the formation of the cyclic intermediate ^{1}W2 (located at –400 kJ/mol). Also in this case, a barrier of 332 kJ/mol from ^{1}W8 must be overcome during the process. The fission of two C-C σ bonds in the ^{1}W2 intermediate, driven by a transition state located 250 kJ/mol below the energy of the reactants, leads to the formation of CO, together with the CH_2CHCH_3 (propene) co-product. Notably, this pathway was not determined in the previous study [32]. Alternatively, two barrierless processes can start from ^{1}W9, leading to the formation of HCO + CH_2CHCH_2 and CH_2CH + CH_2CHO, respectively (Fig. 1).

The interaction of atomic oxygen with the C2 atom of 1,2-butadiene leads to the formation, on the triplet PES, of the ^{3}W1 intermediate, showing a relative energy of

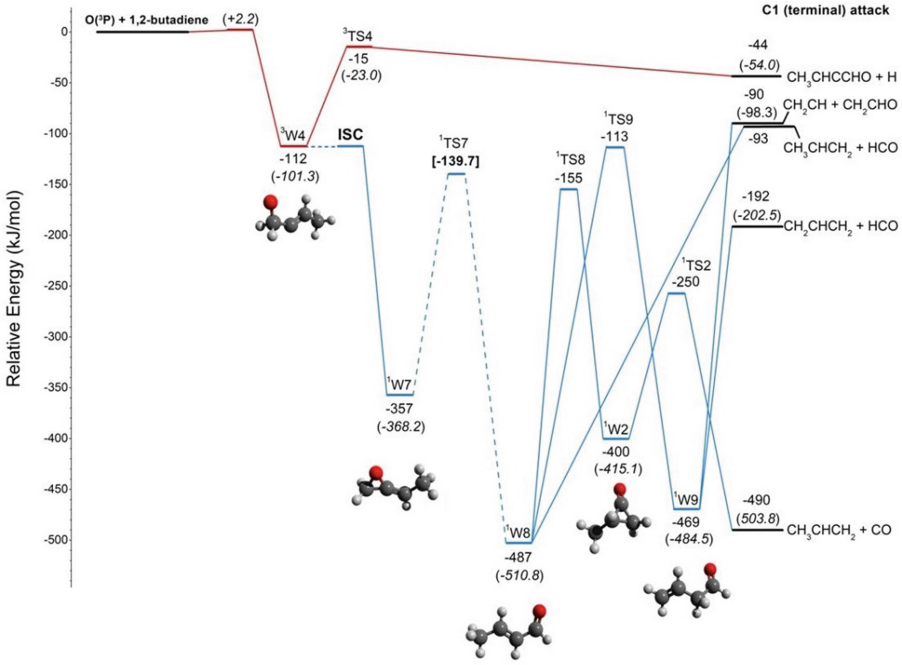

Fig. 1. Potential energy surface of the O(^{3}P) + 1,2-butadiene reaction determined at the CCSD(T)/aug-cc-pVTZ level of theory, by considering the electrophilic attack by O on the terminal carbon (C1). The H channel is formed on the triplet PES, while vinoxy and formyl radical, and CO are generated on the singlet PES via intersystem crossing (ISC). Energy values in parenthesis are for ^{3}TS4 at the CASPT2 level and for all others at the CCSD(T)/CBS/aug-cc-pVTZ level of theory (from ref. 32). The energy barrier for isomerization from ^{1}W7 to ^{1}W8 is here assumed to be the same as that calculated for propylene oxide isomerization to propenal [26] and its value is given between square parenthesis.

–287 kJ/mol (Fig. 2). This intermediate is formed through an entrance submerged barrier, located 1.5 kJ/mol below the reactant energy asymptote (at the CASPT2 level [32]),suggesting the presence of an initial long-range interacting complex, which we were not able to identify at the present level of theory. Furthermore, kinetic calculations [32] have indicated that addition to C2 is the most favoured site of attack, expectedly due to the lack of an entrance barrier and the large stability of the resonantly stabilized ^{3}W1 intermediate. This is similar to what observed in the case of the reaction O(^{3}P) + $CH_2 = C = CH_2$ (allene) where the O addition to C2 leads to the resonantly stabilized oxyallyl intermediate [27]. The triplet diradical ^{3}W1 intermediate can directly undergo dissociation, leading to the formation of the ketene molecule (CH_2CO), together with the CH_3CH radical (ethylidene), overcoming a barrier of 210 kJ/mol (from ^{3}W1) and featuring an exit barrier (^{3}TS1) of 23 kJ/mol with respect to products (see Figs. 2 and 4). At ^{3}TS1 the distance of the dissociating C-C bond is 2.187 Å (see Fig. 4). The global exothermicity of the process is 100 kJ/mol. Also in this case, a competitive reaction channel is represented by the nonadiabatic transition to the singlet PES, through ISC

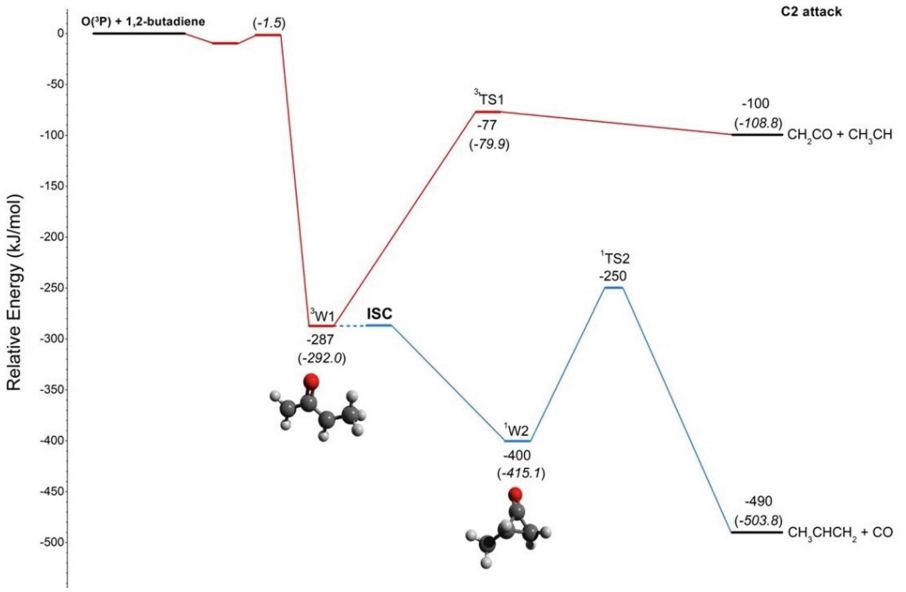

Fig. 2. Potential energy surface of the O(^{3}P) + 1,2-butadiene reaction determined at the CCSD(T)/aug-cc-pVTZ level of theory, by considering the electrophilic attack by O on the central carbon (C2). Energy values in parenthesis are for ^{3}TS1 at the CASPT2 level and for all others at the CCSD(T)/CBS/aug-cc-pVTZ level of theory (from ref. 32). The ketene formation lies on the triplet PES, while propene + CO originates from the singlet PES via ISC.

(presumably around the bottom of ^{3}W1, as in O(^{3}P) + 1,3-butadiene [31]), allowing the formation of the ^{1}W2 cyclic intermediate, located 400 kJ/mol below the reactants. The breaking of two C-C σ bond can then lead to the formation of the CO molecule, together with propene (CH_3CHCH_2), overcoming a barrier of 150 kJ/mol from ^{1}W2 and featuring a very high exit barrier of 240 kJ/mol with respect to products. Clearly, given the lower addition probability of O(^{3}P) to C1 and the high isomerization barrier between ^{1}W7 and ^{1}W8, and between ^{1}W8 and ^{1}W2, we expect that CO + propene formation (channel (3)) is dominantly arising from the C2 addition rather than from the C1 addition.

Similarly, the attack of O(^{3}P) to the C3 atom of 1,2-butadiene shows a submerged transition state, with a relative energy of –1.0 kJ/mol (at the CASPT2 level [32]), leading to the formation of the ^{3}W3 intermediate, characterized by a new C-O σ bond, located 100 kJ/mol below the energy of the reactants (see Fig. 3). The fission of a C-C σ bond leads from ^{3}W3 to the direct formation of the two radical products CH_3 and CH_2CCHO (channel (5)), via an exit barrier of 59 kJ/mol with respect to products. As mentioned for the other two cases (C1 and C2 attack), ISC near the ^{3}W3 minimum is invoked as a competitive reaction pathway (see Fig. 3). Following this approach, the formation of the singlet closed-shell cyclic ^{1}W5 intermediate, showing a relative stability of 372 kJ/mol, can be taken into account. Once formed, ^{1}W5 can isomerize to ^{1}W6, located 503 kJ/mol below the reactants, overcoming a barrier of 268 kJ/mol. The related transition state

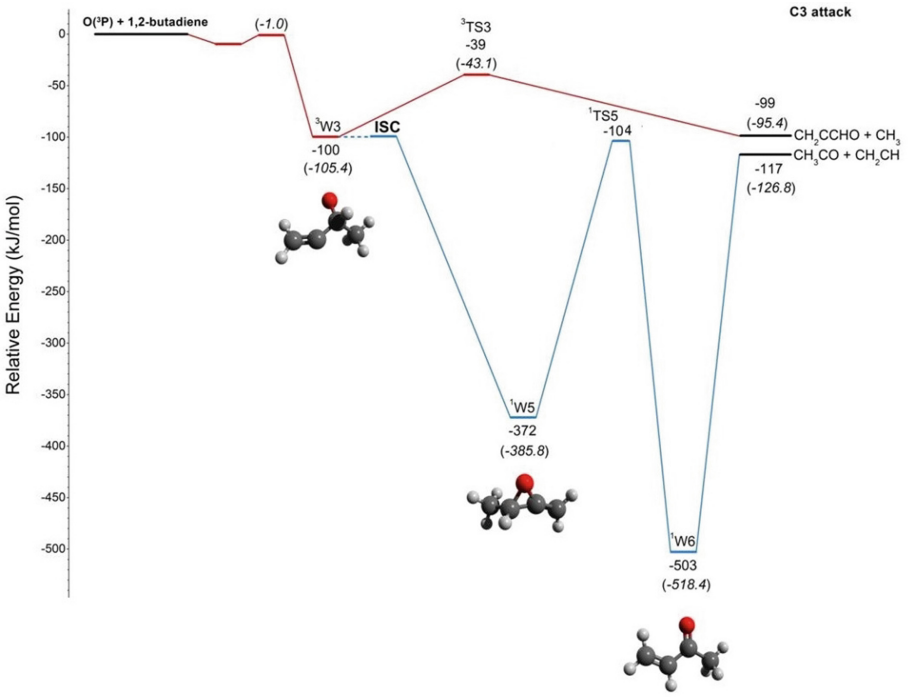

Fig. 3. Potential energy surface of the O(^{3}P) + 1,2-butadiene reaction determined at the CCSD(T)/aug-cc-pVTZ level of theory, by considering the electrophilic attack by O on the C3. Energy values in parenthesis are for ^{3}TS3 at the CASPT2 level and for all others at the CCSD(T)/CBS/aug-cc-pVTZ level of theory (from ref. 32). The CH_3 channel is formed on the triplet PES, while the acetyl radical + vinyl are generated on the singlet PES via ISC.

^{1}TS5 (see Fig. 4) shows the simultaneous breaking of a C-O σ bond and the migration of a hydrogen atom from C2 to C3 of the C_4H_6O intermediate. Finally, the barrierless fission of a C-C σ bond allows the formation of CH_3CO (acetyl) and CH_2CH (vinyl) radical co-products (channel (9)), showing a global exothermicity of 117 kJ/mol. The structures of the most relevant intermediates (^{3}W3, ^{1}W5, ^{1}W6) are shown in Fig. 3, while those of the transition states (^{3}TS3 and ^{1}TS5) are depicted in Fig. 4.

The comparison with the results coming from our previous investigation [32] shows some differences in the values of the energies derived for the different stationary points, the barriers, and the overall channel exothermicities. The explanation of the origin of the observed differences can be ascribed to the use of different levels of theory, especially in the cases of the stationary points that show a strong multi-reference character (such as ^{3}TS4, ^{3}TS1, and ^{3}TS3). In general, the energies of the minima at the present CCSD(T) level are about 3% higher than those obtained at the CCSD(T)-CBS level. Instead, the differences are significantly larger (in percentage) for the exit triplet barriers. Specifically, at the CASPT2 level ^{3}TS4 is at –23.0 kJ/mol, ^{3}TS1 at –79.9 kJ/mol, and ^{3}TS3 at –43.1 kJ/mol, and these values have to be compared with the present CCSD(T) values of –15 kJ/mol, –77 kJ/mol, and –39 kJ/mol, respectively.

It has been demonstrated that, together with ISC, another class of reactions shows a significant multireference character, namely the isomerization of oxyranil singlet intermediates to aldehydes [23, 26, 31]. Such a case is represented by the saddle point identified in the singlet PES related to the C3 attack, linking the ^{1}W5 and ^{1}W6 intermediates, where the calculated energy of ^{1}TS5 (–104 kJ/mol) is expected to be considerably higher than that at the CASPT2 level (see, for instance, ref. 31).

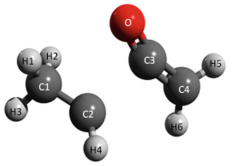

^{3}TS1

Bond	Length
C1-C2	1.460
C2-C3	2.187
C3-C4	1.325
C1-H*	1.09
C2-H4	1.082
C4-H*	1.09
C3-O	1.174

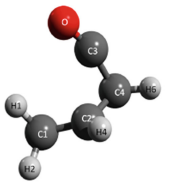

^{1}TS2

Bond	Length
C1-C2	1.490
C2-C4	1.453
C2-C3	2.032
C3-C4	1.470
C1-H1	1.104
C1-H*	1.09
C2-H4	1.081
C4-H*	1.09
C3-O	1.164

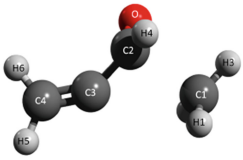

^{3}TS3

Bond	Length
C1-C2	2.134
C2-C3	1.447
C3-C4	1.300
C1-H*	1.08
C2-H4	1.099
C4-H*	1.08
C2-O	1.246

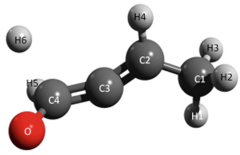

^{3}TS4

Bond	Length
C1-C2	1.501
C2-C3	1.294
C3-C4	1.409
C1-H*	1.08
C2-H4	1.093
C4-H6	1.758
C4-H5	1.100
C4-O	1.255

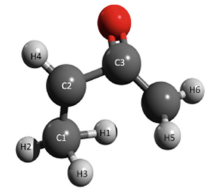

^{1}TS5

Bond	Length
C1-C2	1.386
C2-C4	1.534
C2-C3	1.388
C3-C4	1.470
C1-H1	1.302
C1-H*	1.09
C2-H4	1.081
C4-H*	1.08
C4-H1	1.806
C3-O	1.232

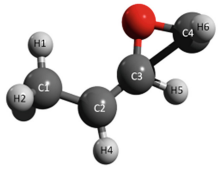

^{1}TS7

Bond	Length
C1-C2	1.495
C2-C3	1.321
C3-C4	1.800
C1-H*	1.08
C2-H4	1.081
C3-H5	1.170
C4-H5	1.536
C4-H6	1.113
C3-O	1.339
C4-O	1.433

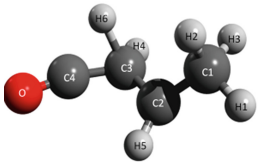

^{1}TS8

Bond	Length
C1-C2	1.496
C2-C3	1.425
C3-C4	1.397
C4-C2	2.299
C1-H*	1.08
C2-H5	1.093
C3-H*	1.081
C4-O	1.156

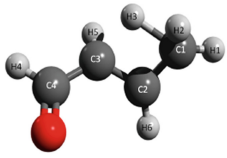

^{1}TS9

Bond	Length
C1-C2	1.391
C2-C3	1.423
C3-C4	1.477
C1-H*	1.09
C1-H3	1.458
C2-H6	1.085
C3-H3	1.492
C3-H5	1.087
C4-H4	1.107
C4-H5	1.278
C3-H5	1.465
C4-O	1.208

Fig. 4. wB97XD/aug-cc-pVTZ optimized geometries (distances in Å) of the labeled transition states identified along the triplet and singlet PESs for the reaction O(^{3}P) + 1,2-butadiene.

Assuming a comparable rate of ISC following C1, C2, and C3 addition, we expect that the most favoured product channel on the singlet PES is the strongly exothermic CO + propene (channel (3)), because the pathway to this product channel is the lowest in energy, while little CH_3CO + C_2H_3, and also HCO + CH_2CHCH_2 (allyl) are expected. These qualitative expectations are corroborated by the preliminary estimates of the experimental BFs (0.49 for CO, 0.027 for CH_3CO, and 0.014 for HCO) [34]. On the triplet PES, given the higher probability of the C2 and C3 additions, we expect mainly CH_2CO (ketene) and CH_3 (methyl) formation, with the H-displacement channel being smaller. Again, these qualitative expectations are in line with our preliminary estimates [34] of the BFs (–0.13 for ketene, –0.15 for methyl, and –0.01 for H). It will be interesting and useful to perform statistical (RRKM/ME) simulations of the product BFs at the collision energy of the CMB experiment. Work in this direction is currently in progress [34].

It is also interesting to compare the dynamics of the $O(^3P)$ + methylallene reaction with that of the simpler, yet closely related $O(^3P)$ + allene reaction. In the oxidation of the prototype of cumulenes (allene), the co-product of carbon monoxide is ethylene [27], while in $O(^3P)$ + 1,2-butadiene the co-product of CO is propene. However, in both reactions the CO main channel originates via ISC from the triplet to the singlet PES. In addition, the energy of the methyl-oxyallyl intermediate (–400 kJ/mol with respect to the energy of the reactants) and the exit barrier (250 kJ/mol for the $O(^3P)$ + 1,2-butadiene reaction and 265 kJ/mol for the $O(^3P)$ + allene reaction) leading to CO formation are comparable in the two reactions. The large stability of the methyl-oxyallyl radical comes from resonance effects, as in the oxyallyl intermediate of the $O(^3P)$ + allene reaction [27]. The probability of the attack to the carbon atom C3 was calculated to be 36.3% by Caracciolo *et al.* [32] and this means that this site attack is the second most important in the title reaction. The attack to the inner carbon by $O(^3P)$ leads to two different, competitive exit channels, namely methyl (CH_3) formation and, via ISC, acetyl (CH_3CO) radical formation. It is interesting to note that this attack site is not present in the reaction between $O(^3P)$ and allene (see refs. 23 and 27), since the allene molecule has three attack sites, but two of these are equivalent (the two terminal carbons, namely C1 and C3). This is the first difference between the two systems, and this will lead to the experimentally observed differences regarding the BFs of the primary products and the extent of ISC (see below). Another important difference between the two systems concerns the PES that describes the attack of atomic oxygen to the terminal carbon (C1) of the unsaturated hydrocarbon. Although this mechanism is the less favoured for both reactions, in the case of the title reaction the PES is somewhat more complicated than that of $O(^3P)$ + allene. In particular, the singlet PES has an exit channel that sees the formation of the vinoxy radical (CH_2CHO) which is not present in the equivalent singlet PES for the $O(^3P)$ + allene system [23, 27] (while it is present on the C_3H_4O triplet PES). In summary, the two reactions that see the attack of $O(^3P)$ on 1,2-butadiene and allene have many similarities but, at the same time, also important differences. For both reactions, the main product channel is represented by the CO molecule formation, which has an experimental BF of 49% and 81.5% for 1,2-butadiene and allene, respectively. In both cases we can assert that this primary product is formed on the singlet PES, after ISC from the entrance triplet PES. For $O(^3P)$ + 1,2-butadiene, both the attack on the

terminal carbon C1 and the attack on the intermediate carbon C2 can give rise to the formation of the CO molecule, but, given the greater probability of the attack to C2 (see ref. 32), we can reasonably assume that most of it is originated after the attack of atomic oxygen on C2, which leads to a resonantly stabilized triplet diradical intermediate.

As previously pointed out, the 1,2-butadiene molecule has one more attack site than the allene molecule, represented by C3, and this entails a differentiation in the global reactivity. In fact, from this attack CH_3 + CH_2CCHO can be formed on the triplet PES, as well as the acetyl (CH_3CO) radical (+ CH_2CH) after ISC to the singlet PES. Experimentally, in $O(^3P)$ + 1,2-butadiene it has been observed that the CH_3 channel has a BF = 0.14 [34], and is the second most important channel under the conditions of the CMB experiment. This essentially entails two interrelated consequences: a smaller extent of ISC in the reaction between $O(^3P)$ and 1,2-butadiene (ISC - 70–75%, [32, 34]) compared to that observed in the reaction between $O(^3P)$ and allene (ISC –85–90%) [27], and therefore a lower yield of the channel that involves the formation of CO for the title reaction (BF = 0.49 vs BF = 0.77 for $O(^3P)$ + allene).

Currently, further calculations are underway in order to perform a statistical estimate of the product BFs, separately on the triplet and singlet PES, as done by Nguyen *et al.* [23] for $O(^3P)$ + allene. The comparison between the experimental BFs and the theoretical BFs on the two distinct PESs should allow us to clarify the detailed overall reaction mechanism of $O(^3P)$ + 1,2-butadiene and to better clarify estimate the extent of ISC for the title reaction.

4 Conclusions

The study at the ab initio CCSD(T)(aug-cc-pVTZ) level of the interaction of $O(^3P)$ with 1,2-butadiene has led to a characterization of the various intermediates and transition states of the triplet and singlet C_4H_6O PESs, as well as to the determination of the energetics of the numerous, competitive product channels of this reaction. Although this level of electronic structure calculations is not fully adequate for determining accurately the energies of the entrance barriers and neither the energy of the inter-conversion and exit barriers exhibiting strong multireference character, as it has emerged from comparisons with the results of previous CCSD(T)(aug-cc-pVTZ)-CBS and CASPT2 calculations on the same system, it nevertheless provides a sufficiently reasonable description of the reactive interaction, which has been useful for a semi-quantitative description of the reaction dynamics, including ISC effects. Higher level calculations, including CBS extrapolation of some of the relevant energies, are in progress. This, together with the previous CASPT2 values of the exit barriers on the triplet PES for this system, should permit in the near future reliable statistical (RRKM/ME) calculations of product BFs, separately on the triplet and singlet PES, to be compared with experimental results of product BFs for nine different observed product channels, as obtained from CMB studies of this reaction. Because some product channels can be rationalized only invoking an important role of ISC, the comparison of experimental and theoretical BFs will shed light also on the extent of ISC in the title reaction.

Acknowledgments. We acknowledge the Italian MUR (Ministero dell'Università e della Ricerca) for "PRIN 2017" funds, project "Modeling and Analysis of carbon nanoparticles for innovative

applications Generated dIrectly and Collected DUring combuSTion (MAGIC DUST)", Grant Number 2017PJ5XXX. We acknowledge support also from Italian MUR, University of Perugia within the program "Department of Excellence-2018–2022-Project AMIS", and "Dipartimento di Ingegneria Civile ed Ambientale" (DICA) of the University of Perugia for allocated computing time within the project "Dipartimenti di Eccellenza 2018–2022".

References

1. Schobert, H.: Chemistry of Fossil Fuels and Biofuels. Cambridge University Press, Cambridge, UK (2013)
2. Frenklach, M., Clary, D.W., Gardiner, W.C., Stein, S.E.: Effect of fuel structure on pathways to soot. Symp. Int. Combust. **21**, 1067–1076 (1988)
3. Gardiner, W.C.: Gas-Phase Combustion Chemistry. Springer, New York (2000). https://doi.org/10.1007/978-1-4612-1310-9
4. Kohse-Höinghaus, K., et al.: Biofuel combustion chemistry: from ethanol to biodiesel. Ang. Chem. Int. Ed. **49**, 3572–3597 (2010)
5. Wayne, R.P.: Chemistry of Atmospheres: An Introduction to the Chemistry of the Atmospheres of Earth, the Planets, and Their Satellites, 3rd edn ACS Publications, Washington, D.C. (2000)
6. Sabbah, H., Biennier, L., Sims, I.R., Georgievskii, Y., Klippenstein, S.J., Smith, I.W.M.: Understanding reactivity at very low temperatures: the reactions of oxygen atoms with alkenes. Science **317**, 102–105 (2007)
7. Occhiogrosso, A., Viti, S., Balucani, N.: An improved chemical scheme for the reactions of atomic oxygen and simple unsaturated hydrocarbons - implications for star-forming regions. MNRAS **432**, 3423–3430 (2013)
8. Simmie, J.M.: Detailed chemical kinetic models for the combustion of hydrocarbon fuels. Progr. Energy Combust. Sci. **29**, 599–634 (2003)
9. Cvetanović, R.J.: Evaluated chemical kinetic data for the reactions of atomic oxygen O(^{3}P) with unsaturated hydrocarbons. J. Phys. Chem. Ref. Data **16**, 261–326 (1987)
10. Casavecchia, P., Leonori, F., Balucani, N.: Reaction dynamics of oxygen atoms with unsaturated hydrocarbons from crossed molecular beam studies: primary products, branching ratios and role of intersystem crossing. Int. Rev. Phys. Chem. **34**, 161–204 (2015)
11. Pan, H., Liu, K., Caracciolo, A., Casavecchia, P.: Crossed beam polyatomic reaction dynamics: recent advances and new insights. Chem. Soc. Rev. **46**, 7517–7547 (2017)
12. Caracciolo, A., et al.: combined experimental and theoretical studies of the O(^{3}P) + 1-butene reaction dynamics: primary products, branching ratios and role of intersystem crossing. J. Phys. Chem. A **123**, 9934–9956 (2019)
13. Blumenberg, B., Hoyermann, K., Sievert, R.: Primary products in the reactions of oxygen atoms with simple and substituted hydrocarbons. Symp. Int. Combust. **16**, 841–852 (1977)
14. Vanuzzo, G., et al.: Isomer-specific chemistry in the propyne and allene reactions with oxygen atoms: CH_3CH + CO versus CH_2CH_2 + CO products. J. Phys. Chem. Lett. **7**, 1010–1015 (2016)
15. Vanuzzo, G., et al.: Reaction dynamics of O(^{3}P) + propyne: I. primary products, branching ratios, and role of intersystem crossing from crossed molecular beam experiments. J. Phys. Chem. A **120**, 4603–4618 (2016)
16. Nguyen, T.L., Vereecken, L., Hou, X.J., Nguyen, M.T., Peeters, J.: Potential energy surfaces, product distributions and thermal rate coefficients of the reaction of O(^{3}P) with C_2H_4(XA_g): a comprehensive theoretical study. J. Phys. Chem. A **109**, 7489–7499 (2005)

17. Nguyen, T.L., Vereecken, L., Peeters, J.: Quantum chemical and theoretical kinetics study of the $O(^3P) + C_2H_2$ reaction: a multistate process. J. Phys. Chem. A **110**, 6696–6706 (2006)
18. Nguyen, T.L., Peeters, J., Vereecken, L.: Theoretical reinvestigation of the $O(^3P) + C_6H_6$ reaction: quantum chemical and statistical rate calculations. J. Phys. Chem. A **111**, 3836–3849 (2007)
19. Balucani, N., Leonori, F., Casavecchia, P., Fu, B., Bowman, J.M.: Crossed molecular beams and quasiclassical trajectory surface hopping studies of the multichannel nonadiabatic $O(^3P)$ + ethylene reaction at high collision energy. J. Phys. Chem. A **119**, 12498–12511 (2015)
20. Rajak, K., Maiti, B.: Trajectory surface hopping study of the $O(^3P) + C_2H_2$ reaction dynamics: effect of collision energy on the extent of intersystem crossing. J. Chem. Phys. **140**, 044314 (2014)
21. Cavallotti, C., et al.: Relevance of the channel leading to formaldehyde + triplet ethylidene in the $O(^3P)$ + propene reaction under combustion conditions. J. Phys. Chem. Lett. **5**, 4213–4218 (2014)
22. Li, X., Jasper, A.W., Zádor, J., Miller, J.A., Klippenstein, S.J.: Theoretical kinetics of O + C_2H_4. Proc. Combust. Inst. **36**, 219–227 (2017)
23. Nguyen, T., Peeters, J., Vereecken, L.: Quantum chemical and statistical rate study of the reaction of $O(^3P)$ with allene: O-addition and H-abstraction channels. J. Phys. Chem. A **110**, 12166–12176 (2006)
24. Casavecchia, P., Capozza, G., Segoloni, E., Leonori, F., Balucani, N., Volpi, G.G.: Dynamics of the $O(^3P) + C_2H_4$ reaction: Identification of five primary product channels (vinoxy, acetyl, methyl, methylene, and ketene) and branching ratios by the crossed molecular beam technique with soft electron ionization. J. Phys. Chem. A **109**, 3527–3530 (2005)
25. Fu, B., et al.: Intersystem crossing and dynamics in $O(^3P) + C_2H_4$ multichannel reaction: experiment validates theory. In: Proceedings of the National Academy of Sciences (U.S.A.), vol. 109, pp. 9733–9738 (2012)
26. Leonori, F., et al.: Experimental and theoretical studies on the dynamics of the $O(^3P)$ + propene reaction: primary products, branching ratios, and role of intersystem crossing. J. Phys. Chem. C **119**, 14632–14652 (2015)
27. Leonori, F., Occhiogrosso, A., Balucani, N., Bucci, A., Petrucci, R., Casavecchia, P.: Crossed molecular beam dynamics studies of the $O(^3P)$ + allene reaction: primary products, branching ratios, and dominant role of intersystem crossing. J. Phys. Chem. Lett. **3**, 75–80 (2012)
28. Leonori, F., Balucani, N., Capozza, G., Segoloni, E., Volpi, G.G., Casavecchia, P.: Dynamics of the $O(^3P) + C_2H_2$ reaction from crossed molecular beam experiments with soft electron ionization detection. Phys. Chem. Chem. Phys. **16**, 10008–10022 (2014)
29. Casavecchia, P., Leonori, F., Balucani, N., Petrucci, R., Capozza, G., Segoloni, E.: Probing the dynamics of polyatomic multichannel elementary reactions by crossed molecular beam experiments with soft electron-ionization mass spectrometric detection. Phys. Chem. Chem. Phys. **11**, 46–65 (2009)
30. Vanuzzo, G., et al.: Crossed-Beams and theoretical studies of the $O(^3P, {}^1D)$ + benzene reactions: primary products, branching fractions, and role of intersystem crossing. J. Phys. Chem. A **125**, 8434–8453 (2021)
31. Cavallotti, C.; Della Libera, A.; Recio, P.; Caracciolo, A.; Balucani, N.; Casavecchia, P.: Crossed-beam and theoretical studies of multichannel nonadiabatic reactions: branching fractions and role of intersystem crossing for $O(^3P)$ + 1,3-butadiene. Faraday Discuss. (2022). In press. https://doi.org/10.1039/D2FD00037G
32. Caracciolo, A., et al.: Crossed molecular beams and theoretical studies of the $O(^3P)$ + 1,2-butadiene reaction: dominant formation of propene + CO and ethylidene + ketene molecular channels. Chin. J. Chem. Phys. **32**, 113–122 (2019)
33. NIST Chemistry WebBook, Gaithersburg, MD: National Institute of Standards and Technology (2002)

34. Vanuzzo, G., et al.: Work in progress
35. Chai, J.D., Head-Gordon, M.: Systematic optimization of long-range corrected hybrid density functionals. J. Chem. Phys. **128**, 084106 (2008)
36. Chai, J.D., Head-Gordon, M.: Long-range corrected hybrid density functionals with damped atom–atom dispersion corrections. Phys. Chem. Chem. Phys. **10**, 6615–6620 (2008)
37. Jr Dunning, T.H.: Gaussian basis sets for use in correlated molecular calculations. I. the atoms boron through neon and hydrogen. J. Chem. Phys. **90**, 1007–1023 (1989)
38. Woon, D.E., Jr Dunning, T.H.: Gaussian basis sets for use in correlated molecular calculations. III. the atoms aluminum through argon. J. Chem. Phys. **98**, 1358–1371 (1993)
39. Kendall, R.A., Jr Dunning, T.H., Harrison, J.R.: Electron affinities of the first-row atoms revisited. systematic basis sets and wave functions. J. Chem. Phys. **96**, 6796–6806 (1992)
40. Gonzalez, C., Schlegel, H.B.: An improved algorithm for reaction path following. J. Chem. Phys. **90**, 2154–2161 (1989)
41. Gonzalez, C., Schlegel, H.B.: Reaction path following in mass- weighted internal coordinates. J. Phys. Chem. **41**, 5523–5527 (1990)
42. Frisch, M. J., et al.: Gaussian 09, Rev. A.02, Gaussian, Inc., Wallingford, CT (2009)
43. Werner, H.-J., Knowles, P.J., Knizia, G., Manby, F.R., Schütz, M.: Molpro: a general-purpose quantum chemistry program package. WIREs Comput. Mol. Sci. **2**, 242–253 (2012). https://doi.org/10.1002/wcms.82
44. Werner, H.-J., et al.: The Molpro quantum chemistry package. J. Chem. Phys. **152**, 144107 (2020). https://doi.org/10.1063/5.0005081
45. Cavallotti, C., et al.: Theoretical study of the extent of intersystem crossing in the O(^{3}P) + C_6H_6 reaction with experimental validation. J. Phys. Chem. Lett. **11**, 9621–9628 (2020)